White Paper

Phases of moiré Chern insulators

… probed with attocube nanopositioners, cryostats and microscopes

Rajarshi Bhattacharyya[1], Evgeny Redekop[2] and Mirko Bacani[1]

[1]attocube systems AG, 85540 Haar, Germany
[2]Department of Physics, University of California at Santa Barbara, Santa Barbara CA 93106, USA

Abstract

Moiré bilayers of van der Waals (vdW) materials are a perfect playground for studying the properties of Chern insulators. We present here a selection of remarkable results achieved with attocube systems technology in labs of attocube customers with emphasis on integer and fractional moiré Chern insulators (MCIs) in vdW bilayers: Scanning magnetometry of an integer MCI $MoTe_2/WSe_2$ shows that its magnetization can be flipped with a very low current [1], which is appealing for utilization in energy-efficient magnetic memories. A magneto-optical study of the same heterostructure discovered a valley-coherent nature of the quantum anomalous Hall state in this material [2]. A scanning single electron transistor (SET) study [3] established the high field flavor phase diagram of the magic angle twisted bilayer graphene (MATBG), identified earlier as an integer MCI at high field [4]. Scanning magnetometry also reveals the mosaic of MCIs with different Chern numbers induced by local variations in the Berry curvature as a function of the filling factor [5]. Moreover, MATBG can also host fractional Chern insulating states (FCIS) even in low magnetic fields $B < 12$ T [6]. Finally, FCIS that survive in $B = 0$ have been identified magneto-optically in twisted bilayer $MoTe_2$ using trion sensing [7].

1. Introduction

The discoveries of a superconducting phase and a tuneable Mott-like insulating phase in MATBG [8] have established moiré bilayers as an intricate playground for the realization of strongly-correlated electronic and topological quantum phenomena. One way of producing a 2D superlattice is to stack two identical sheets of material and rotationally misalign them in case of twisted bilayer graphene or twisted bilayer $MoTe_2$. The other way is to stack two layers with slight difference in lattice constant like in case of $MoTe_2/WSe_2$. The resulting moiré superlattice exhibits a remarkably flat energy band separated from the others by large single-particle energy gaps. This gives rise to strongly interacting electrons which are essential for observing exotic quasiparticle excitations, like anyons in the regime of fractional quantum Hall effect (FQHE).

In his seminal work [9], Duncan Haldane has changed the paradigm that B is necessary to create quantum Hall-like states with flat band dispersion and strong electron-electron interactions. He showed that breaking of time reversal symmetry can be accomplished by introducing next-nearest-neighbour hopping (NNNH) between the lattice sites (K and K´ points in the momentum space). This is exactly the case that we encounter in moiré bilayers, where a mini-Brillouin zone (MBZ) in momentum space enhances the NNNH. The reciprocal structure of MBZ in real space is the moiré superlattice, which is usually 10 - 100 times larger than the atomic spacing. Therefore, moiré bilayers exhibit an exotic topological phenomenon when the Hall resistance is quantized, and longitudinal resistance is zero even at $B = 0$. This effect is called quantum anomalous Hall (QAH) effect, and materials exhibiting QAH effect are a type of topological insulators commonly referred to as Chern insulators (CIs). Their topological properties at $B = 0$ and relatively high temperatures (~0.1 - 10 K) compared to magnetically doped topological insulators make moiré bilayers a paragon system for studying the interplay between topology and strongly-correlated electronic phenomena like superconductivity and Mottness.

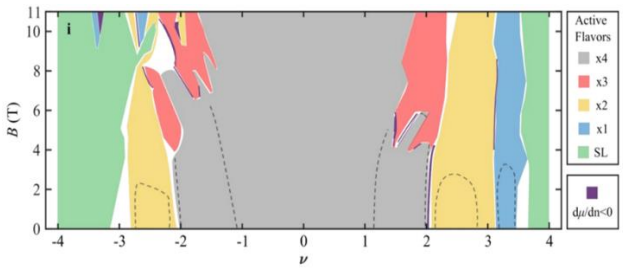

Fig 1: Phases of Chern insulator in MATBG, corresponding to 4 possible combinations of spin and valley flavours. Green area is where all spin and valley values are simultaneously active. Filling factor ν is number of electrons per moiré superlattice site. Dashed lines engulf regions of non-anomalous quantum Hall effect [3].

Such a versatile system calls for experiments that can probe its phases and their connection with precision. This is where attocube comes into the picture with measurement setups and tools that are designed to perform such complex measurements with great precision. Below we would like to present a few remarkable results which provide deeper insight into properties of Chern insulator phases in moiré bilayers, and which have been achieved with attocube equipment in the labs of attocube customers. We focus on scanning probe and magneto-optical measurements, which are known to be delicate, and where precise positioning along with low vibration and minimal drift in cryogenic variable temperature and high magnetic field environments are of the utmost importance.

2. Current-driven magnetic switching in a moiré Chern magnet

Moiré Chern magnets have been realized as a platform for engineering low-current magnetic switches that can have

applications in magnetic memories. In moiré heterostructures, broken time-reversal symmetry coupled with strong Coulomb repulsion at certain rational electron/hole fillings can give rise to Chern insulator state. The group of Andrea Young (University of California at Santa Barbara, USA) in collaboration with the group of Kin Fai Mak and Jie Shan (Cornell University, USA) [1] aimed to understand the underlying mechanism of the low-current magnetization switching, which had been demonstrated earlier in twisted mono-bilayer graphene [10].

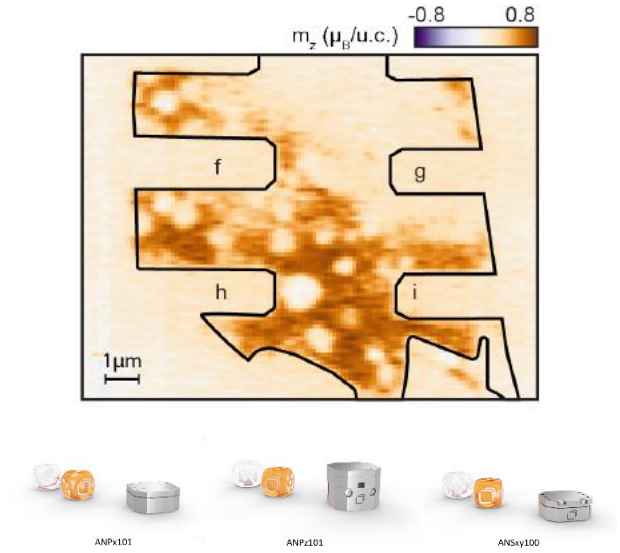

Fig 2. 2D map of magnetization at QAH phase measured with a nanoSQUID-on-tip sensor using attocube nanopositioners ANPx101, ANPz101 and ANSxy100 [1]

In this study a trilayer moiré superlattice consisting of a $MoTe_2$ bilayer and a WSe_2 monolayer stacked with 60° relative crystal axis alignment was taken into a QAH state by applying a strong perpendicular electric field, and the hole filling was kept at filling factor of $\nu = -1$, at 1.6 K. The observed Chern magnet state having nearly quantized anomalous Hall effect and vanishingly small longitudinal resistance at B = 0 was studied using transport methods and nanoSQUID-on-tip (nSOT) microscopy to investigate the hysteretic current behaviour.

A nanoSQUID fabricated from indium at the apex of a quartz tube, attached to a piezoelectrically-driven tuning fork with magnetic field sensitivity of 15 nT/Hz$^{1/2}$, was used to image magnetic ordering in real space, which is responsible for the underlying mechanism of current switching. A modulation of the global back gate voltage at a frequency of 3 kHz resulted in modulation of the fringing magnetic field δB stemming from the magnetic order picked up by the nSOT. Precise correlation between reversal of magnetic domain and applied current was found when local change in magnetization was imaged at I_{SD} = 670 nA. A current-driven domain magnetization reversal, observed by measuring the local magnetic response to a small AC current, identified the mechanism of an intrinsic spin Hall effect disturbing magnetic order and exerting a torque on the equilibrium moment which leads to local magnetization reversal of the Chern magnet. Magnetization switching in this system requires a record low current density of $j < 10^3$ Acm^{-2}, which is significantly less than the lowest observed thus far in spin-orbit torque systems.

attocube nanopositioners ANPx101, ANPz101 and ANSxy100 were used to perform the measurements.

3. Spontaneous spin-polarized and valley-coherent Chern states

The QAH effect in MATBG comes with a valley-polarized ground state as a consequence of interaction-driven valley symmetry breaking. However, broken inversion symmetry and strong spin-orbit interaction in stacked TMD heterolayers can give rise to independent Chern bands in each layer. It is an interesting question whether the valley Chern bands remain polarized or become coherent as a result of interlayer coupling, as the system is taken to a QAH state. The group of Jie Shan and Kin Fai Mak (Cornell University, USA) in collaboration with the group of Tony Heinz (Stanford University, USA) investigated this question in an AB-stacked $MoTe_2/WSe_2$ moiré bilayer using layer-resolved and helicity-resolved optical spectroscopy and transport measurements [2].

Optical selection rules pertaining to the coupling of attractive valley polaron with the helicity of the probing circularly-polarized light determine whether valley polarization or coherence would occur between the stacked layers. The TMD bilayer is first taken to a Mott-insulator state with filling of one hole per lattice site (v = -1). Applying a perpendicular electric field then causes a topological phase transition and drives the system into the CI state.

With the system being in the CI state, layer- and helicity-resolved optical reflectance contrast (RC) is measured while sweeping B from -8 T to 8 T as function of energy. At B = 0, attractive valley polaron responded mostly to σ^- helicity of the excitation in both layers. This confirms the valley coherence along with spin polarization. At $B \neq 0$, the spin and magnetic moment alignment in both layers shows the same response with respect to excitation helicity.

Further study by magnetic circular dichroism (MCD) as a function of B revealed that about 45% and 60% of the full spin polarization is sufficient for quantized Hall resistance in WSe_2 and $MoTe_2$ layers respectively, at B = 0. Moreover, a temperature-dependent MCD study identifies spin texture and

the effect of thermal fluctuations. The temperature dependence of the spin susceptibility agrees very well with the Curie-Weiss law, thereby supporting a very unexpected result of canted spin texture with non-zero in-plane component in CI state of the bilayer. This result opens further avenues for understanding magnetic ground state of CI phase in AB-stacked TMD moiré bilayers.

An attoDRY2100 and a confocal setup were used to obtain a low-temperature (1.6 K) and low-vibration environment.

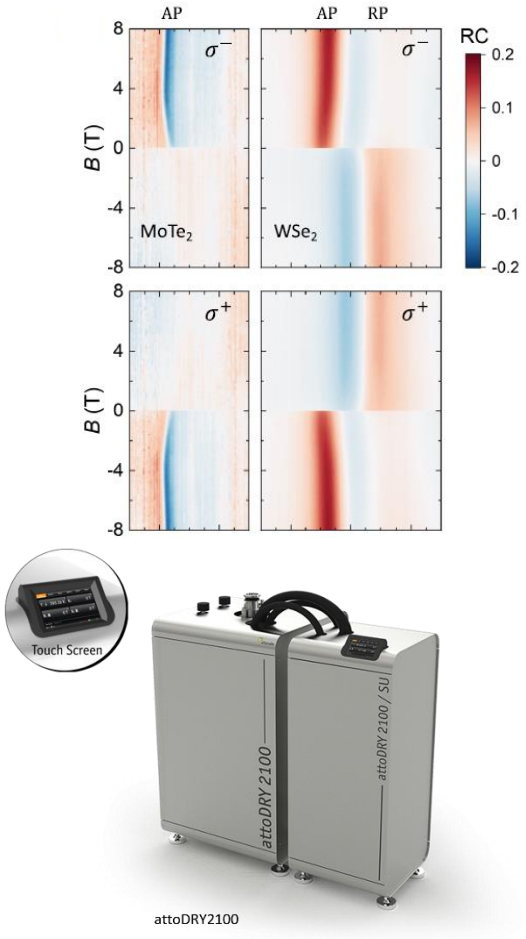

Fig 3. Magnetic field dependence of reflectance contrast spectrum w.r.t helicity (σ^+ or σ^-) of $MoTe_2/WSe_2$ bilayer measured in attoDRY2100 [2].

4. Identifying strongly correlated topological phases in MATBG

Competing topological states occupying fractal Hofstadter energy subbands in the presence of a strong perpendicular *B* and varying electronic occupancy in moiré bilayers is an extremely interesting topic for physicists. Spin or valley flavour occupancy in MATBG further enriches the picture, when one looks into the topological phase transitions. Collaboration between the groups of Benjamin Feldman, Zhi-Xun Shen and Steven Kivelson (Stanford University, USA) performed a complete mapping of the underlying Hofstadter energy spectrum and thermodynamic phase transition among those competing topological states using scanning single-electron tunnelling (SET) microscopy to measure local inverse electronic compressibility $d\mu/dn$ in the range T = 0.33 – 1.7 K [3].

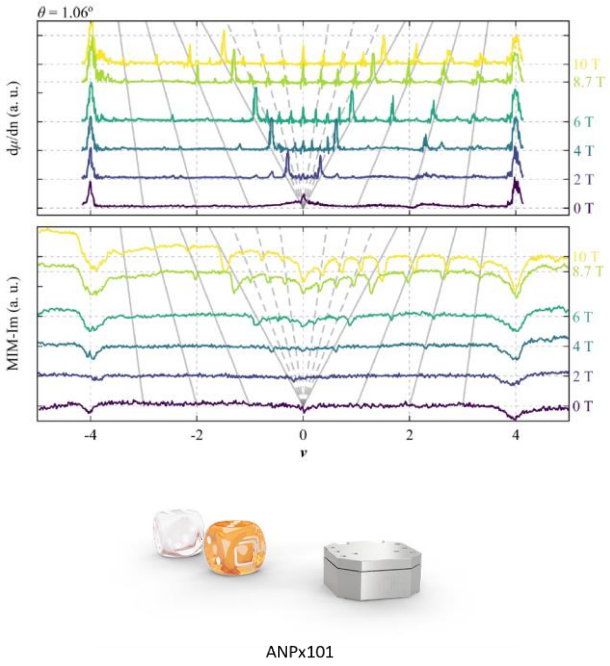

Fig 4. Inverse compressibility from scanning SET and local conductivity measurements from microwave impedance microscopy (MIM) are compared. Local conductivity mapping via MIM measurements were performed using attocube nanopositioners ANPx101 [3].

Applying perpendicular magnetic field (0-11 T) and tuning the moiré filling $\nu = -4 \rightarrow 4$, the Wannier diagram was obtained that shows a number of gapped incompressible states that spans quantum Hall states having Landau levels (LL) originating from charge neutrality point (CNP), all the way to novel correlated Chern Insulator (CI) states at high field that were never reported before. Different CI states have been observed to intersect at specific regions in the Wannier diagram, that indicate competition between single-particle and interaction driven symmetry breaking. Independent measurement of scanning microwave impedance microsocopy (MIM) revealed the robustness of certain CI states satisfying $|s| + |t| = 4$ (Diophantine tuples) at high magnetic fields and at 450 mK. Dips in the imaginary part of the MIM signal identified decrease in local conductivity, strengthening further the existence of the CI

states in (ν, B) space. The thermodynamic many-body energy level $\mu(n, B)$ (Fermi energy) obtained by integrating local compressibility was used to experimentally determine interacting Hofstadter energy spectrum, where phase transitions can be clearly distinguished by looking at vHs (van-Hove singularity)-like feature of the density of states.

The central result of this work is the construction of the interacting Hofstadter phase diagram of MATBG. A mechanism for symmetry breaking based on flavour is proposed which stands in a good agreement with experimental data. Such unified picture of different phases of CI in MATBG is immensely useful understanding the underlying mechanism of phase transitions dictated by flavour polarization as a function of density and applied magnetic field.

attocube nanopositioners ANPx101 were used to perform the microwave impedance microscopy measurements.

5. Imaging local variation of Chern number in MATBG

CIs are characterized by the Chern number – a topological invariant resulting from extended Berry curvature over the gapped energy band under condition of broken time reversal symmetry. However, theoretical proposals show that a local variation of Chern number is expected to occur in moiré bilayers due to spatially varying substrate potential. Groups of Eli Zeldov (Weizmann Institute of Science, Israel) and Dmitri Efetov (ICFO, Spain) probed this hypothesis using an intentionally nonaligned (with the hBN substrate) MATBG sample, by mapping equilibrium local orbital magnetism over a range of metallic and gapped states (as a function of moiré filling) [5].

Transport experiments were carried yielding pronounced and non-trivial hysteresis in the transverse resistance nearby $\nu = 1$, indicating the presence of orbital magnetism and anomalous Hall effect (AHE). Magnetic mapping was performed using an indium SQUID-on-tip (SOT) scanning at a height of ~160 nm on top of the sample surface and in the presence of B = 50 mT applied perpendicularly to the sample. Images were obtained by measuring the change in local magnetic signal induced by modulating backgate voltage. The data reveals a number of patches throughout the sample with different Chern numbers.

Local differential magnetization data revealed complex pattern of isolated patches having positive (paramagnetic-like) and negative (diamagnetic-like) response to the external magnetic field for $\nu = 0.966$. The emergence and development of the pattern is clearly visible over a range of filling factors around $\nu = 1$. The observed mosaic pattern (named Chern mosaic by the authors) of the two types of patches is proposed to have the following two possible mechanisms: i) spontaneous sublattice symmetry breaking near $\nu = 1$ resulting from spatially varying potential due to incommensurate hBN substrate potential with the graphene moiré lattice, ii) twist angles between graphene layers, and between hBN layer with respect to the adjacent graphene layer can create nearly commensurate moiré lattices resulting into a periodic sublattice polarization. This coupled with strain, structural relaxation and disorder can give rise to non-homogeneous local Chern bands resulting in a Chern mosaic pattern. This result is suggestive of the ubiquity of such topological disorder in MATBG devices, unless an intentionally aligned MATBG sample is fabricated against the hBN substrate.

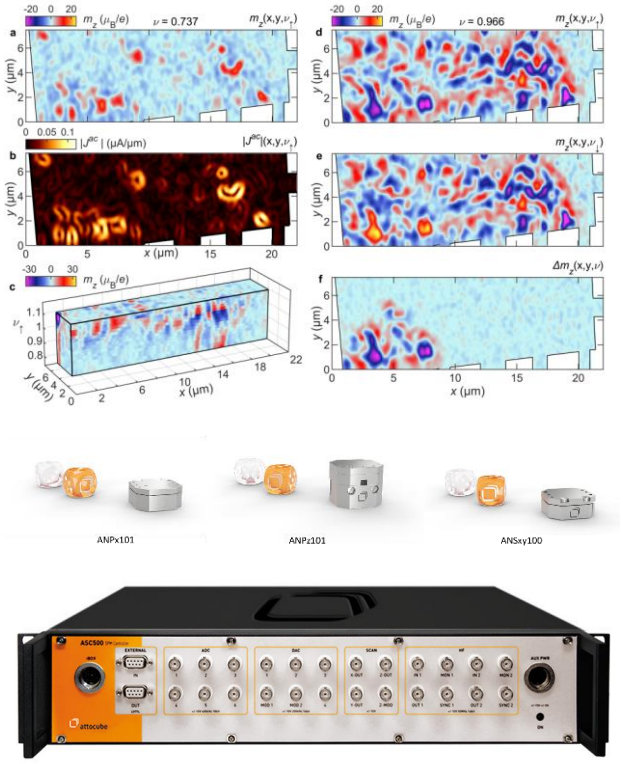

Fig 5. Imaging local magnetization and reconstructed equilibrium current density across MATBG sample with nanoSQUID sensor using attocube nanopositioners ANPx101, ANPz102 and ANSxy100. Scan control and data acquisition has been performed using attocube scanning probe microscopy controller ASC500 [5].

Here, attocube scanning probe microscopy controller ASC500 together with nanopositioners ANPx101, ANPz102 and ANSxy100 were used to obtain magnetic imaging data.

6. Observation of fractional Chern insulator states in MATBG

Anyons hosted by strongly-correlated 2D electronic systems (e.g., FQHE at high magnetic fields) are believed to be extremely

useful for performing fault-tolerant topological quantum computing, owing to their exotic exchange statistics. In 2D moiré systems, fractional Chern bands are supposed to host anyons at very low magnetic field, theoretically even at $B = 0$. In this work, the authors have reported observation of fractional Chern insulator (FCI) states in MATBG, at B as low as 5 T.

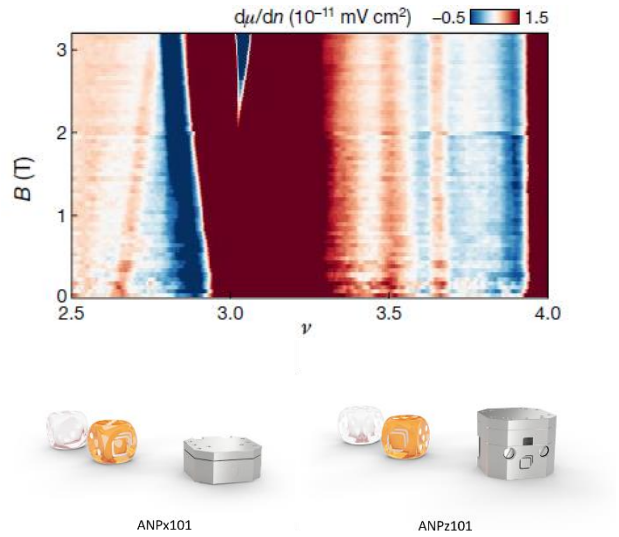

Fig 6. Mapping charge density waves by inverse electronic compressibility with scanning SET sensor using attocube nanopositioners ANPx101 and ANPz101 [6].

The groups of Amir Yacoby (Harvard University, USA) and Pablo Jarillo-Herrero (MIT, USA) have performed inverse compressibility measurements (measuring equilibrium $d\mu/dn$) using a scanning single electron transistor (SET) setup on a MATBG sample with a twist angle of ~1.06° [6]. The obtained Wannier diagram (gapped states as a function of moiré filling ν and applied perpendicular magnetic field B) shows a variety of linearly dispersing incompressible states classified by a tuple (t,s) that satisfies Diophantine equation $\nu = \frac{t\phi}{\phi_0} + s$. Out of five different classes of incompressible states that include integer quantum Hall states, charge density waves (CDW) and symmetry-broken CI states, the most fascinating are FCI states that take only fractional values of both t and s. A total of eight FCI states have been observed sweeping the filling factor from -4 to 4 and magnetic field up to 12 T.

Two FCI states, (2/3, 10/3) and (1/3, 11/3), that are observed all the way down to 5 T, are particularly intriguing. These two states, which can be thought of as lattice analogues of 1/3 and 2/3 FQHE states, are observed in the filling regime $3 < \nu < 4$. Energy gaps of both states (obtained by integrating $\frac{d\mu}{dn}$ with respect to electron density and multiplying with expected quasiparticle charge e/3) reached 50 ± 20 μeV, that roughly agrees with the theoretical prediction. Further investigation into understanding the competition between CDW and FCI states revealed that Berry curvature inhomogeneity, stemming from interlayer tunnelling between AA-stacked and AB-stacked regions, has an upper bound, which determines the phase boundary between these competing states. That explains why magnetic field was required to observe FCI states in the MATBG sample.

Six other FCI states have been observed mostly in the hole doping regime, $-3 < \nu < 1$, at higher magnetic fields. Among those six states, FCI states having no FQHE analogue were identified, in particular the ones having co-prime denominator of t and s. This observation opens routes to study exotic phases of Chern insulators exclusively in MATBG systems.

attocube cryogenic nanopositioners ANPx101 and ANPz101 were used in performing local inverse electronic compressibility measurements.

7. Observation of fractional Chern states at $B = 0$

An experimental signature of the long-sought FCI states at B = 0 in moiré bilayers has been demonstrated in this work. Based on the observation of electrically tuneable ferromagnetic states with broken time-reversal symmetry [11] in rhombohedral-stacked MoTe2 twisted bilayer, the authors investigated the system in the hole-doping regime using an optical detection method.

The group of Xiaodong Xu (University of Washington, USA) used reflective magnetic circular dichroism (RMCD) to study the phase space of ferromagnetic states around lattice filling $\nu = -1$ & -2/3 as a function of applied perpendicular electric and magnetic fields [7]. An ubiquitous magnetic phase was confirmed spanning from $\nu = -1.2$ to $\nu = -0.4$. The observation of ferromagnetism was further supported by measuring RMCD hysteresis loops.

To determine and characterize gapped states, the authors employed a technique of sensing trion photoluminescence (PL) [12]. The spectrally integrated PL intensity as function of magnetic field and doping (ν) clearly shows a linear dispersion for $\nu = -1$ & -2/3 with slopes of -1 and -2/3, respectively. It also shows a weak dispersive feature for $\nu = -3/5$ with C = -3/5 at low B values. The most exciting observation is the survival of the C = -2/3 state all the way down to $B = 0$, paving the way for the realization of Abelian anyons at $B = 0$ and coupling them to superconducting circuits. Furthermore, the topological phase transitions were observed for both C = -1 and C = -2/3 CIs by applying perpendicular electric field.

The attoDRY2100 cryostat was used here to obtain a low-temperature (1.6 K) and low-vibration environment for the

attocube systems AG, Eglfinger Weg 2, 85540 Haar, Germany

measurements. An attoCFM I was used to perform the optical measurements.

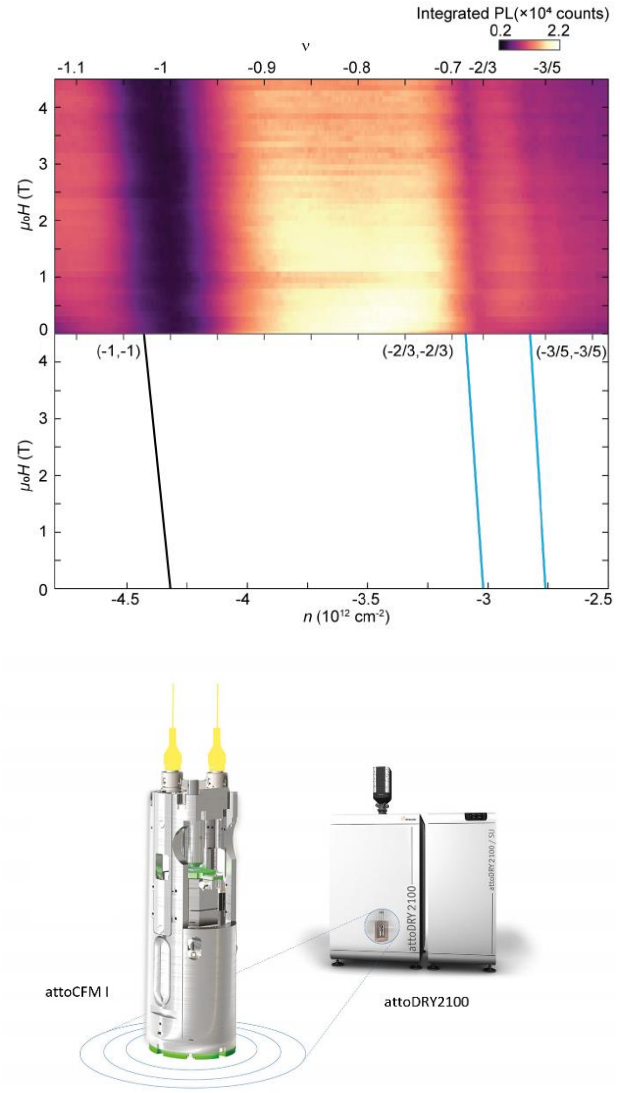

Fig 7. Optical Landau fan diagram with integer and fractional QAH states in twisted $MoTe_2$ bilayer, revealed by utilizing an attoCFM I and an attoDRY2100 [7].

8. Conclusion

Quantum Hall effect is a paragon for topological manifestations in quantum physics and has hence always attracted a lot of interest. Yet, experimental studies thereof have not been easy due to the requirements for extreme environment, like high magnetic fields, ultra-low temperatures and ultra-high vacuum. However, realization of Chern insulators in 2D materials has enabled fundamental studies of quantum Hall effect at moderate magnetic fields, and in the absence of both ultra-low temperatures and ultra-high vacuum. attocube cryogenic equipment makes such moderate environmental requirements readily available and has already enabled scientific impact in the field of Chern insulators, as exemplified in this white paper.

Cryogenic nanopositioning and nanorotating setups of attocube systems are suitable for nanoscale studies of Chern insulators because they provide supreme stability, and are accompanied by ultra-low-vibrations cryostats. These cryogenic scanning setups include confocal microscopes and various scanning probe microscopes, ranging from magnetic force microscope (MFM), SQUID microscope and nitrogen vacancy (NV) microscope, to single-electron-transistor (SET) microscope, microwave impedance microscope (MIM) and quantum twisting microscope (QTM).

References

[1] C.L. Tschirhart, E. Redekop, L. Li, T. Li, S. Jiang, T. Arp, O. Sheekey, T. Taniguchi, K. Watanabe, M.E. Huber, K.F. Mak, J. Shan and A.F. Young, *Nature Physics* **19**, 807 (2023)

[2] Z. Tao, B. Shen, S. Jiang, T. Li, L. Li, L. Ma, W. Zhao, J. Hu, K. Pistunova, K. Watanabe, T. Taniguchi, T.F. Heinz, K.F. Mak and J. Shan, *Physical Review X* **14**, 011004 (2024)

[3] J. Yu, B.A. Foutty, Z. Han, M.E. Barber, Y. Schattner, K. Watanabe, T. Taniguchi, P. Phillips, Z.-X. Shen, S.A. Kivelson and B.E. Feldman, *Nature Physics* **18**, 825 (2022)

[4] K.P. Nuckolls, M. Oh, D. Wong, B. Lian, K. Watanabe, T. Taniguchi, B.A. Bernevig and A. Yazdani, *Nature* **588**, 610 (2020)

[5] S. Grover, M. Bocarsly, A. Uri, P. Stepanov, G. Di Battista, I. Roy, J. Xiao, A.Y. Meltzer, Y. Myasoedov, K. Pareek, K. Watanabe, T. Taniguchi, B. Yan, A. Stern, E. Berg, D.K. Efetov and E. Zeldov, *Nature Physics* **18**, 885 (2022)

[6] Y. Xie, A.T. Pierce, J.M. Park, D.E. Parker, E. Khalaf, P. Ledwith, Y. Cao, S.H. Lee, S. Chen, P.R. Forrester, K. Watanabe, T. Taniguchi, A. Vishwanath, P. Jarillo-Herrero and A. Yacoby, *Nature* **600**, 439 (2021)

[7] J. Cai, E. Anderson, C. Wang, X. Zhang, X. Liu, W. Holtzmann, Y. Zhang, F. Fan, T. Taniguchi, K. Watanabe, Y. Ran, T. Cao, L. Fu, D. Xiao, W. Yao and X. Xu, *Nature* **622**, 63 (2023)

[8] Y. Cao, V. Fatemi, S. Fang, K. Watanabe, T. Taniguchi, E. Kaxiras and P. Jarillo-Herrero, *Nature* **556**, 43 (2018)

[9] F.D.M. Haldane, *Physical Review Letters* **61**, 2015 (1988)

[10] H. Polshyn, J. Zhu, M.A. Kumar, Y. Zhang, F. Yang, C.L. Tschirhart, M. Serlin, K. Watanabe, T. Taniguchi, A.H. MacDonald and A.F. Young, *Nature* **588**, 66 (2020)

[11] E. Anderson, F.-R. Fan, J. Cai, W. Holtzmann, T. Taniguchi, K. Watanabe, D. Xiao, W. Yao and X. Xu, *Science* **381**, 325 (2023)

[12] A. Popert Y. Shimazaki, M. Kroner, K. Watanabe, T. Taniguchi, A. Imamoğlu and T. Smoleński, *Nano Letters* **22**, 7363 (2022)